

## Numerical Analysis of Forces in Negative Bending Region of Steel-Concrete Composite Beams

<sup>1, 2</sup> Wang Yang, <sup>2</sup> Li Tian

<sup>1</sup> School of Civil Engineering, Zhengzhou University,  
Zhengzhou, Henan 450002, China

<sup>2</sup> School of Civil Engineering, Taizhou Vocational & Technical College,  
Taizhou, Zhejiang 318000, China

*Received: 26 January 2014 /Accepted: 7 March 2014 /Published: 30 April 2014*

**Abstract:** Steel-concrete composite frame is a kind of structure consisting of a combination of steel and concrete members. In the connection between beams and columns, if the column section size is too large, connecting problems between steel beams and columns are introduced into these structures. For connecting problems between additional longitudinal reinforcements of the steel-concrete composite beam and concrete columns filled with square steels, through numerical analysis on the connection forms of additional longitudinal reinforcements, this paper explored the influence of different distributions of additional longitudinal reinforcements on forces in negative bending region of steel-concrete composite beams. In this paper, a finite element model of the edge across part of steel-concrete composite frames is established, to examine the elastic and plastic ultimate bearing capacity of the negative bending region. Results indicate that, in the negative bending region of steel-concrete composite beams, there will be adverse conditions of concrete in tension and steel beams in compression, resulting in reduction of the stiffness of the negative bending region of the beams. In this situation, concrete panels are easy to crack, affecting the normal function of the structure. Copyright © 2014 IFSA Publishing, S. L.

**Keywords:** Steel-concrete composite member, Negative bending region, Finite element model, Reinforcements.

### 1. Introduction

Steel-concrete composite beams are made of two materials of steel and concrete; through shear connectors, steel beams and concrete structural members are connected into a whole composite structure. With advantages such as high rigidity, high capacity, and high energy capacities, steel-concrete composite beams has been widely used in high-rise buildings and other long-span structures [1, 2]. For connecting nodes of steel-concrete composite beams and steel-concrete columns, if the column section size is too large, connecting problems between longitudinal reinforcements within the effective

width of the concrete flange plate and steel concrete columns are introduced into these structures. In order to solve such problems, a number of approaches, such as opening holes in pillars, additional connecting disks, additional sleeve connections, have been developed in construction [3]. The mechanical properties, such as stiffness, bearing capacity, destruction forms, and crack distribution, of the negative bending region, will be affected by different connection forms [4].

A number of experimental and theoretical studies have been conducted by many researchers. To sum up, three methods have been proposed: the first one is the classical linear elastic theory presented by

Newark, Siess and Viest [5] proposed, which assumes that all three parts of the composite beam are in linear elastic stage; the second one is the rigid-plastic analysis method proposed by Yam and Chapman [6, 7], in which the three parts of the composite beam are considered as total plastic, and this method is mainly used to calculate the ultimate bearing capacity of composite beams; the third one is the "mixing" method proposed by Oehlers and Sved [8], in which the connectors plastic, while the steel beams and concrete composite beam flanges are considered as total plastic. At present, researches on composite beams are mainly focused on the ultimate bearing capacity of shear connectors, ultimate bearing capacity of bending sections, deformation and stiffness of the beam, shear strength of the beam, influence of shrinkage and creep of concrete on combination beams, cracks of negative bending region of steel-concrete composite beams, performance of continuous composite beams, stiffness calculation, interface slippage of the composite beams, etc [9]. Since the 1990s, with the popularization of composite beams, further in-depth researches have been implemented on composite beams. In 1998, Y. C. Wang gave out formulas for calculating the deflection of partial shear connection composite beams through the conduction of experimental researches [10]. In 2004, Amadio et al [11] studied the effective width of steel-concrete composite beams, and proposed calculating method to analyze the effective width when the composite beam is destructed under the effect of negative moment. In practice, the mechanical characteristics of the two materials can be fully exploited using composite beams. However, when using continuous composite beams, the adverse conditions of concrete in tension and steel beams in compression will be emerged [12]. In this case, premature cracks will appear in the negative bending region, thereby reducing the cross-section strength and stiffness; and because of the cracks [13], corrosion on reinforcements maybe occur, reducing the durability of the structures. In this paper, a finite element model of the edge across part of steel-concrete composite frames is established to examine the elastic and plastic ultimate bearing capacity of the negative bending region, providing effective basis for the delay and control of the emergence of cracks in the negative bending region.

## 2. The Establishment of Finite Element Model

ABAQUS finite element analysis consists of a series of steps, which constitute the entire process of the analysis of physical problems. A complete ABAQUS analysis process is implemented in the following order: creating a discrete geometric shape; specifying material properties and model assembly; applying loads and boundary conditions; meshing;

setting analysis step, analysis type and output requirements; running the program; outputting data.

### 2.1. The Basic Theory of the Finite Element Analysis

Under the effect of external loads, it is an eigenvalue problem for the emergence of an equilibrium state besides the original equilibrium state, which is called eigenvalue buckling analysis. Generally, buckling loads and the corresponding buckling modes are calculated in eigenvalue buckling analysis. Eigenvalue buckling analysis is linear elastic analysis. Due to the predicted critical buckling load of the eigenvalue buckling analysis is generally larger than the practical buckling load, the results of eigenvalue buckling analysis are used as preliminary assessment of nonlinear buckling analysis, rather than being directly used in actual structural analysis. When a structure is in flexion state, displacement will be increased greatly as a small growth in load. Then, the finite element equilibrium equation can be written as:

$$([K] + \lambda[S])\{\psi\} = 0, \quad (1)$$

where  $[K]$  is the elastic  $\lambda$  is the eigenvalue, i.e. proportion factor of the given load;  $[S]$  is the stress stiffness matrix;  $\{\psi\}$  is the displacement eigenvector. In ABAQUS, eigenvalue buckling analysis is realized through the Buckle function under the Linear Perturbation in the setup of step.

In ABAQUS/Standard, the nonlinear question under the effect of static loads can be analyzed using Static general and Static Riks under the menu of General in the setup of step, the corresponding algorithms are Newton-Raphson algorithm and arc-length method respectively. Newton-Raphson algorithm is used to solve function  $f(x) = 0$  by the first several items of the Taylor expansion. The biggest advantage of this algorithm is that the function shows square convergence in the vicinity of its single root. This method is also used to solve the roots or complex roots.

When solving nonlinear equation  $f(x) = 0$ , the main idea of Newton-Raphson algorithm is to approximately liberalize the nonlinear equation. The Taylor expansion of  $f(x)$  around  $x_0$  is:

$$f(x) = f(x_0) + (x - x_0)f'(x_0) + (x - x_0)^2 \frac{f''(x_0)}{2!} + \dots, \quad (2)$$

Take the linear part of the Taylor expansion as the approximate linear equation of the nonlinear equation  $f(x) = 0$ , and then solve it.

The basic idea of arc-length method is to introduce a parameter equivalent to the length of the arc to be solved geometrically, and the incremental step is controlled through controlling the arc length. The basic equation of the arc-length method is as follows:

$$\{\Delta u\}^T \{\Delta u\} + \Delta \lambda^2 \varphi \{P\}^T \{P\} = \Delta l^2, \quad (3)$$

where  $\{\Delta u\}$  is the displacement increment;  $\{P\}$  is the vector of the external load;  $\Delta \lambda$  is the load factor increment;  $\varphi$  is the load ratio factor;  $\Delta l$  is the given arc length.

When defining plasticity in ABAQUS true stress and true strain must be adopted; while for most experiments, data of materials are often given by nominal stress and nominal strain. In this case, nominal stress (strain) of the plastic material must be transformed into true stress (strain). The relationship between nominal stress and true stress is written as:

$$\sigma = \sigma_{nom} (1 + \varepsilon_{nom}), \quad (4)$$

The relationship between nominal strain and true strain is written as:

$$\varepsilon = \ln(1 + \varepsilon_{nom}), \quad (5)$$

where  $\varepsilon$  is the true strain;  $\varepsilon_{nom}$  is the nominal strain;  $\sigma$  is the true stress;  $\sigma_{nom}$  is the nominal stress.

## 2.2. ABAQUS Model for the Negative Bending Region of Steel-concrete Composite Beams

Composed of the two materials of steel beams and concrete, steel-concrete composite beams are generally in a complex stress state due to the interaction of the two materials in the loading process. In order to analyze the static properties of steel-concrete composite beams, the constitutive model of steel and concrete and the mechanical model of the interface between the two materials must be established.

Steel is an ideal homogeneous material; the mechanical properties in tension and compression are basically of the same for small deformation. For simplicity, the stress-strain curve of steel is always idealized, and a number of stress-strain models have been presented for steels with different properties. The following constitutive models are widely used in practice: ideal elastic-plastic model, three-fold model, whole curve model and bilinear model. Under multi-axial stress state, we use the Von Mises yield

criterion to determine the yield of the steel specimens in this paper. Von Mises yield criterion is applied to metal materials, the equivalent stress is:

$$\sigma_c = \sqrt{0.5[(\sigma_1 - \sigma_2)^2 + (\sigma_2 - \sigma_3)^2 + (\sigma_3 - \sigma_1)^2]}, \quad (6)$$

where  $\sigma_1$ ,  $\sigma_2$  and  $\sigma_3$  are the three principal stresses. When the equivalent stress  $\sigma_c$  exceeds the yield stress  $f_y$ , plastic deformation will occur.

In this work, the concrete damage plasticity model combined in ABAQUS is adopted to discuss the damage of the concrete flange. Based on a large number of experimental and theoretical studies, a number of concrete constitutive models have been proposed, such as linear-elastic model, nonlinear-elastic model, plastic model, etc. In the case of uniaxial compression, the stress-strain expression of concrete can be written as:

Ascent stage:

$$\sigma_c = [\alpha_\varepsilon \frac{\varepsilon}{\varepsilon_0} + (3 - 2\alpha_\varepsilon) (\frac{\varepsilon}{\varepsilon_0})^2 + (\alpha_\varepsilon - 2) (\frac{\varepsilon}{\varepsilon_0})^3] f_c \quad \varepsilon < \varepsilon_0, \quad (7)$$

Decline stage:

$$\sigma = \frac{\frac{\varepsilon}{\varepsilon_0}}{\alpha_d (\frac{\varepsilon}{\varepsilon_0} - 1)^2 + \frac{\varepsilon}{\varepsilon_0}} f_c \quad \varepsilon_0 \leq \varepsilon \leq \varepsilon_u, \quad (8)$$

where  $f_c$  is the compressive strength of the concrete;  $\varepsilon_0$  is the strain corresponding to the peak stress;  $\alpha_\varepsilon$  and  $\alpha_d$  are the parameters for the ascent stage and decline stage of the uniaxial compressive stress-strain curve respectively.

In the case of uniaxial tension, the stress-strain expression of concrete can be written as:

Ascent stage:

$$\sigma = E \varepsilon \quad \varepsilon < \varepsilon_t, \quad (9)$$

Decline stage:

$$\sigma = \frac{\frac{\varepsilon}{\varepsilon_t}}{\alpha_t (\frac{\varepsilon}{\varepsilon_t} - 1)^{1.7} + \frac{\varepsilon}{\varepsilon_t}} f_t \quad \varepsilon > \varepsilon_t, \quad (10)$$

where  $f_t$  is the tension strength of the concrete;  $\varepsilon_t$  is the strain corresponding to  $f_t$ ;  $\alpha_t$  is the parameters for the decline stage of the uniaxial tension stress-strain curve.

In the simulation of this paper, the tested steel beam and concrete flange are connected together

using the merge command. In addition, surface-to-surface contact is adopted for all the contact between the steel beam and concrete flange. According to the Penalty friction formula, assume no friction exists between the steel beam and concrete flange, i.e. the friction coefficient is equal to 0. The direct effect between the two materials is considered as small sliding. For normal effect, "hard" contact feature is taken to describe the interaction. In addition, "tension stiffening" has been introduced to consider the interaction between steel and concrete.

### 3. Simulation Results

#### 3.1. Material Properties and Loading Program

A typical connection is selected as the simulation object in this paper. The specimens the connector between the additional longitudinal reinforcement steel in the flange plate and the square steel concrete column. All specimens are made of Q345B steel, and the manual welding rods are E50 type. The designed strength grade of both the square steel concrete and the flange plate is C30; the type of steel bars distributed in the plate is HRB400 with diameter of 8 mm; the steel mesh is 200 mm×200 mm; the type of additional longitudinal reinforcements is HRB400 with diameter of 16 mm; pegs are made of ML15 steel. The measured mean value of the concrete strengths 38.5 N/mm<sup>2</sup>; the axial compressive strength is 25.5 N/mm<sup>2</sup>; the tension strength is 2.53 N/mm<sup>2</sup>. The average yield strength of the beam is 389 N/mm<sup>2</sup>; the average tensile strength is 517 N/mm<sup>2</sup>; the yield ratio is 0.75. The average yield strength of the 16mm additional longitudinal reinforcements is 482 N/mm<sup>2</sup>; the average tensile strength is 705 N/mm<sup>2</sup>. The average yield strength of the 8mm steel bars is unknown; the average tensile strength is 741 N/mm<sup>2</sup>. The measured strengths of steel bars and steel plates all meet the strength requirements of the specification.

Loading control method is adopted for loading process; the loading process contains the following steps:

- 1) Prior to the formal loading, the specimen is pre-loaded with 30 %~40 % of the cracking load of the composite beam.

- 2) Start the formal loading process. Load level is controlled by load increment (5 ken each step) before the emergence of cracks.

- 3) After cracking, increase 10 KN per step; when the load-deformation relation shows good linearity, increase 20 KN per step.

- 4) When inflection point occurs for the load-displacement curve of the specimen, the specimen enters non-linear state; in this case, load increment can be reduced according to the stable state.

- 5) With the increase of load, if the phenomenon of unstable load, continuous unloading, large cracks

(crack width greater than 5 mm), or large deformation occur, the specimen is believed destroyed.

#### 3.2. Force Analysis of the Negative Bending Region of Composite Beams

Fig. 1 and Fig. 2 show the experimental and calculated stress values of steel bars in composite beams under concentrated loads respectively, where the calculated values are obtained using the elastic theory. The curves show that the calculated and agree well with measured values. It can be seen from the figures that the stress of steel bars in composite beams can be obtained through strain differential analysis of the interface.

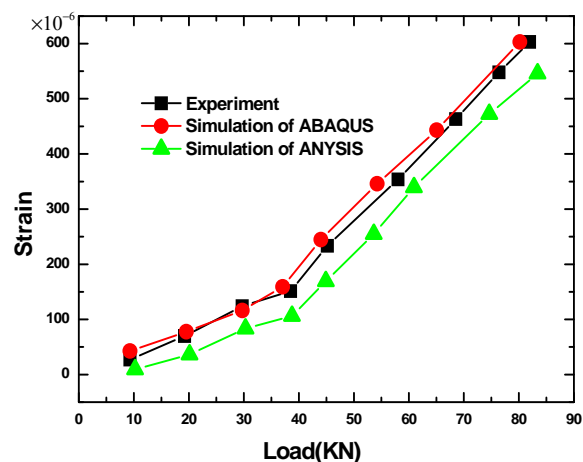


Fig. 1. The relationship between the load and strain of test Full beam without pegs.

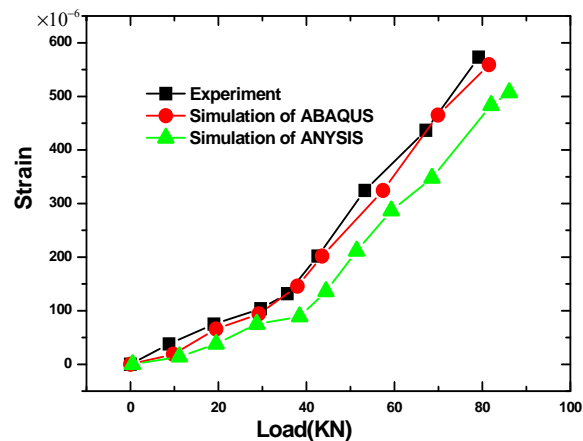


Fig. 2. The relationship between the load and strain of test Full beam layout pegs.

Fig. 3 and Fig. 4 show the comparison of the stress of steel bars in negative bending region of steel-concrete composite beams obtained by ABAQUES modeling and experimental values. It can

be seen from the figure that numerical and experimental values are in good consistent, indicating that the use of finite element program to build composite beam model to simulate the loading process is credible.

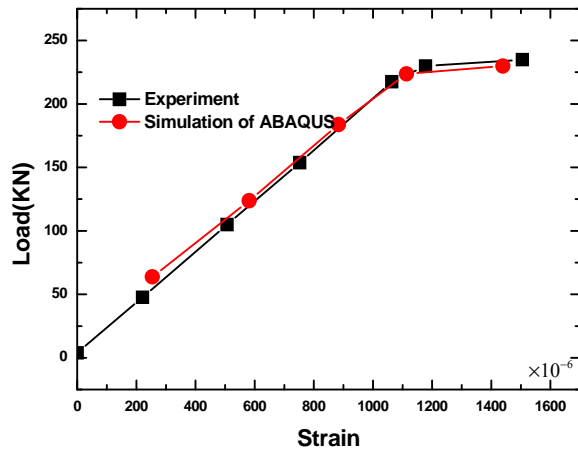


Fig. 3. The relationship between the load and strain of top-level test Full beam without pegs.

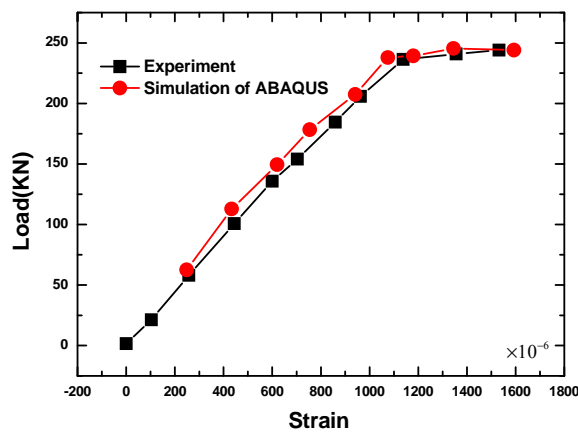


Fig. 4. The relationship between the load and strain of top-level test Full beam layout pegs.

Ultimate bearing capacity obtained from the model and experiment values are listed in Table 1. As can be seen from the table, ultimate bearing capacity obtained from the model is smaller than theoretical values. In the process of ABAQUES modeling, cohesive effect between the concrete and steel beams are ignored except the stud force, which will increase the shear slip amount between steel beams and concrete and impact the ultimate bearing capacity results of the composite beam. However, the maximum difference between the two hasn't exceeded 2.5 % of the experimental value, so the ABAQUES model is able to reflect the carrying capacity of the beam correctly.

The load P-vertical deformation  $\Delta$  curves are shown in Fig. 5. The specimens are in elastic state before the appearance of cracks, and the deformation

is in linear relationship with load. As the load increases, cracks start to emerge, the specimen stiffness is gradually degraded, and the load-deformation curves become nonlinear.

**Table 1.** Ultimate bearing capacity obtained from the simulation model and experiment values.

Ultimate bearing capacity	Simulation model	Experiment values
Full beam layout pegs	248	256
Full beam without pegs	238	251

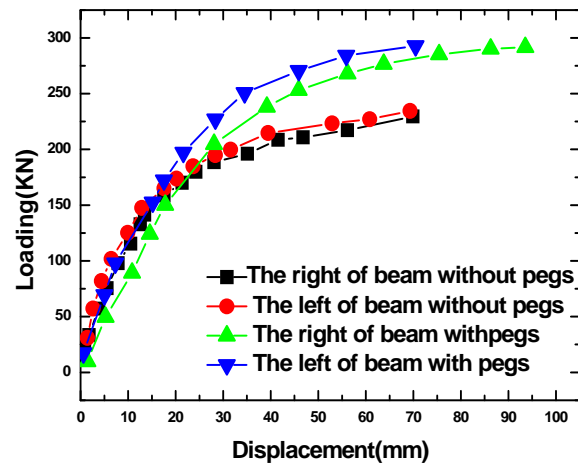


Fig. 5. The curves of the load and strain at different point.

The stress distribution in longitudinal reinforcements of the concrete flange plate at 100 mm is shown in Fig. 6. For small loadings, due to the effect of shear lag and cracking in the concrete plate, stress distribution in longitudinal reinforcements is uneven; with the increase of load and the development of cracks in the concrete plate, stress distribution becomes even, strain tends to be equal within the cross-section, and the shear lag effect becomes significantly smaller.

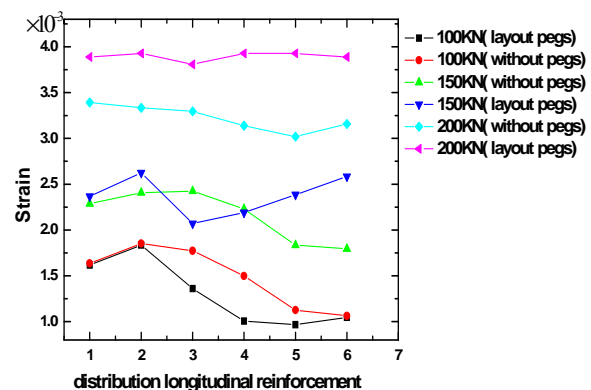


Fig. 6. The strain of distribution longitudinal reinforcement at the same section.

Since cracks appear at the edge of the flange plate at first, tensile stress is withstood mainly by the additional longitudinal reinforcements in the region. As the further increase of the load, cracks will run through the flange plate at the edge, and the distribution of the tensile stress in additional longitudinal reinforcements tends to be more uniform. When the ultimate load is reached, the tensile strain of additional longitudinal reinforcements exceeds the yield strain of steel; therefore, it is reasonable to design the ultimate bearing capacity assuming the whole cross-section be plastic.

#### 4. Conclusions

In this paper, a finite element model is established for the edge-across part of steel-concrete composite frames, and the elastic and plastic ultimate bearing capacities of the negative bending region are examined. Results indicate that, in the negative bending region of steel-concrete composite beams, there will be adverse conditions of concrete in tension and steel beams in compression, resulting in reduction of the stiffness of the negative bending region of the beams. In this situation, concrete panels are easy to crack, affecting the normal function of the structure. Due to the concrete plate in negative bending region of steel-concrete composite beams bears the effect of tension, cracks will appear at this region even for small loads; and with the increase of the load, more cracks will be generated. Therefore, measures should be applied for concrete plates in the beam-column connecting area of continuous composite beams or frames, to control the development of cracks to meet the control requirements of normal use. The below flanges of steel beams in negative bending region of steel-concrete composite beams bear the effect of pressure. When combination design is adopted, the pressure effect on the lower flange will be enhanced; so the phenomena of plastic buckling is more prone to occur at the below flanges when the steel beam is in rotation. So in the design of beam-column connection, the plastic evolution in the negative bending region should be appropriately restricted.

#### Acknowledgement

The work was supported by Zhejiang Provincial Natural Science Foundation of China (Y1100387), Zhejiang Construction research (2012095), and the project leader in professional leaders of professional vocational colleges of Zhejiang Provincial (lj2013143)

#### References

- [1]. J. Deng, M. M. Lee, S. Li, Flexural strength of steel-concrete composite beams reinforced with a prestressed CFRP plate, *Construction and Building Materials*, Vol. 25, Issue 1, 2011, pp. 379-384.
- [2]. A. Zona, G. Ranzi, Finite element models for nonlinear analysis of steel-concrete composite beams with partial interaction in combined bending and shear, *Finite Elements in Analysis and Design*, Vol. 47, Issue 2, 2011, pp. 98-118.
- [3]. M. Dilella, A. Morassi, Vibrations of steel-concrete composite beams with partially degraded connection and applications to damage detection, *Journal of Sound and Vibration*, Vol. 320, Issue 1, 2009, pp. 101-124.
- [4]. M. Dawood, S. Rizkalla, E. Sumner, Fatigue and overloading behavior of steel-concrete composite flexural members strengthened with high modulus CFRP materials, *Journal of Composites for Construction*, Vol. 11, Issue 6, 2007, pp. 659-669.
- [5]. N. M. Newmark, C. P. Siess, Viest I.M., Tests and analysis of composite beams with incomplete interaction, *Proc Soc Exp Stress Anal*, Vol. 9, Issue 1, 1951, pp. 75-92.
- [6]. A. Fam, C. MacDougall, Amr Shaat, Upgrading steel-concrete composite girders and repair of damaged steel beams using bonded CFRP laminates, *Thin-Walled Structures*, Vol. 47, Issue 10, 2009, pp. 1122-1135.
- [7]. A. Zona, M. Barbato, J. P. Conte, Nonlinear seismic response analysis of steel-concrete composite frames, *Journal of Structural Engineering*, Vol. 134, Issue 6, 2008, pp. 986-997.
- [8]. O. Mirza, B. Uy, Behaviour of headed stud shear connectors for composite steel-concrete beams at elevated temperatures, *Journal of Constructional Steel Research*, Vol. 65, Issue 3, 2009, pp. 662-674.
- [9]. C. Pellegrino, E. Maiorana, C. Modena, FRP strengthening of steel and steel-concrete composite structures: an analytical approach, *Materials and Structures*, Vol. 42, Issue 3, 2009, pp. 353-363.
- [10]. Y. C. Wang, Deflection of steel-concrete composite beams with partial shear interaction, *Journal of Structural Engineering*, Vol. 124, Issue 10, 1998, pp. 1159-1165.
- [11]. A. Zona, Ranzi, Finite element models for nonlinear analysis of steel-concrete composite beams with partial interaction in combined bending and shear, *Finite Elements in Analysis and Design*, Vol. 47, Issue 2, 2011, pp. 98-118.
- [12]. G. Vasdravellis, B. Uy, E. L. Tan, B. Kirkland, Behaviour and design of composite beams subjected to negative bending and compression, *Journal of Constructional Steel Research*, Vol. 79, 2012, pp. 34-47.
- [13]. Srouf Nofal, et al, Effects of material variability on the ductility of composite beams and overstrength coefficients, *Earthquake Engineering & Structural Dynamics*, Vol. 42, Issue 7, 2012, pp. 953-972.